Journal of Applied Mathematics and Computation, 2024, 8(1), 59-67
https://www.hillpublisher.com/journals/JAMC/
ISSN Online: 2576-0653
ISSN Print: 2576-0645

Dynamic Modeling and Simulation of Mobile Robot Under Disturbances and Obstacles in an Environment

Vesna Knights[1,*], Olivera Petrovska[2]

[1]Faculty of Technology and Technical Science, University “St. Kliment Ohridski”, Bitola, Republic of North Macedonia.
[2]Faculty of Technical Science, Mother Teresa University, Skopje, Republic of North Macedonia.

How to cite this paper: Vesna Knights, Olivera Petrovska. (2024) Dynamic Modeling and Simulation of Mobile Robot Under Disturbances and Obstacles in an Environment. *Journal of Applied Mathematics and Computation*, 8(1), 59-67.
DOI: 10.26855/jamc.2024.03.007

Received: February 28, 2024
Accepted: March 27, 2024
Published: April 26, 2024

***Corresponding author:** Vesna Knights, Faculty of Technology and Technical Science, University “St. Kliment Ohridski”, Bitola, Republic of North Macedonia.

Abstract

This paper aims to develop a mathematical model of a mobile robot, utilizing a deductive approach to create a versatile model applicable to various tasks and adjusted for specific scenarios. The study employed dynamic modeling and simulation analysis to investigate the posture stabilization of a mobile humanoid upper-body robot amidst diverse disturbances and cart movements. Control strategies were implemented, and simulations were conducted using MATLAB to assess the robot's stability and performance under various scenarios. The findings demonstrate the robot's successful navigation through various obstacle configurations, albeit encountering challenges at higher speeds. The study emphasizes the relevance of mobile robots in human-centered environments, underscoring the importance of balance, stability, and accuracy in robot functioning. This research provides new insights and directions for future studies in the field of mobile robotics. It highlights the practical implications of developing humanoid robots capable of navigating complex environments, contributing to advancements in service robotics. By developing a mathematical model and simulating the performance of a wheeled humanoid robot in obstacle environments, this study offers original contributions to the literature. It underscores the significance of addressing challenges related to robot posture, robustness, and obstacle avoidance in enhancing the functionality of humanoid robots in real-world applications

Keywords

Dynamics modeling, Mathematical modeling, Mobile robots, Simulations, Guidance and control

1. Introduction

Humanoid robots represent a significant advancement in robotics technology, aiming to help in everyday life [1-5]. In that context, humanoid robots operate in human environments with obstacles, such as homes, stores, and hospitals, and the selection of appropriate robot drives plays a crucial role in achieving the desired performance [6, 7]. Exploring the kinematic and dynamic equations governing the motion of the wheeled mobile base is essential for understanding the robot's behavior during different maneuvers and tasks [8]. Moreover, the role of robots extends beyond domestic settings, as demonstrated in applications such as robots for safety and health at work" [9-11], where they play a crucial role in hazardous situations. Robot helps to nonstop monitoring for the purpose of contributing to the field of IoT security in “Methods for Detection and Prevention of Vulnerabilities in IoT Systems” [12].

The dynamic modeling and simulation analysis of humanoid robots are crucial for understanding their stability, performance, and interaction with the environment. Applications of robots are going further and further advanced, including the guidance and control system for a platoon of autonomous mobile robots [13].

Dynamical modeling of the mobile robot is a partial implementation of the classical "flier approach" in humanoid robotics [14], and presents a unique challenge due to its upper-body configuration. In the past few years, a new expression has been established—anthropometric [15, 16]. Additionally, one of the famous methods of dynamical modeling in obstacle avoidance algorithms for mobile robots, using the “Potential Fields Method” [17].

As the field of robotics continues to evolve, research efforts focus on enhancing path-planning techniques to improve mobile robot navigation [18, 19]. Furthermore, the concept of Zero Moment Point (ZMP) has played a pivotal role in analyzing dynamic balance and stability in humanoid robots [20-22]. Recent studies have extended the application of ZMP to achieve dynamically stable walking movements by ensuring its position within the convex torso formed by all contact points between the robot's feet and the ground [23, 26].

Overall, this research addresses critical challenges in humanoid robotics, advancing our understanding of posture stabilization and motion planning for mobile humanoid robots and their movement in obstacles environments.

2. Methods

2.1 Design and Objective

This paper focuses on the dynamic modeling and simulation analysis of the mobile robot, a humanoid upper-body robot, particularly in the context of posture stabilization under various disturbances and obstacle cart movements. The dynamic modeling and simulation analysis aims to check to what extent the mobile robot can stand the disturbance resulting from different cart movements and disable the overturning of the robot during some common tasks and obstacles. Cart movements are restricted in the consideration of which are relevant to the humanoid robot working in a human environment with obstacles.

The selection of the robot drives is essential for the simulation results and therefore for establishing the limits of the robot acting The ECCEROBOT[1] uses Maxon products, and for this study, the following motors and gearboxes were chosen:

- Waist joints are used: 148877 DC motor RE40 48V and 203116 Gearbox GP42C 15:1
- Shoulder joints are used: 268193 DC motor RE30 12V and 326664 Gearbox GP32HP 51:1
- Neck, elbow, and wrist joints use 118637 DC motor RE13 12v and 110315 Gearbox GP13A 67:1

2.2 Mathematical Modeling

The “classical” dynamic model that considers the joint torques as the controls and relates them to joint motions. The concept of the “flier” approach, is derived for humanoid robots [14, 16]. Unlike full humanoid robots, the mobile robot is a humanoid robot only a part of the upper body. The system configuration of a mobile robot is: main body (head, pelvis, torso, and arms), contact, and moving ground (cart). The system configuration and the structure of the mechanism used for the simulation in Matlab is presented at Figure 1.

The idea of the ‘*flier’* approach is to consider the humanoid freely flying in space and then to introduce contact with environmental objects in order to model the imposed motion task. This applies to any motion task: walking and running, manipulation, sporting motions, etc.

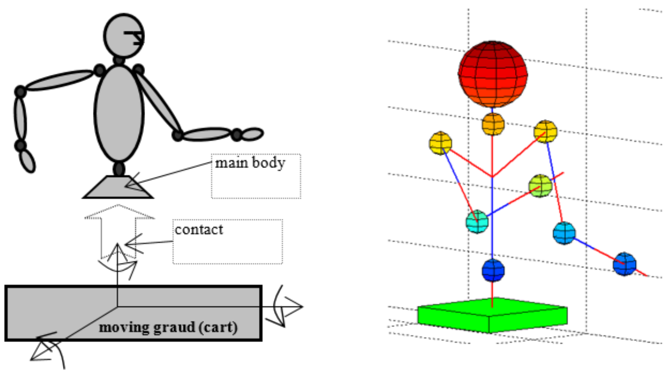

Figure 1. The system configuration and simulation model.

[1] EU FP7 project: Embodied Cognition in a Compliantly Engineered Robot (www.eccerobot.org).

Following the flier concept, starts the dynamic analysis from the free-flying model. If robot has n single-rotation joints (n=20 for the configuration under investigation), then its position is defined by a vector of dimension N=6+n:

$$Q_{N\times 1}\,[X \quad q]^T = [x \quad y \quad z \quad \theta \quad \varphi \quad \psi \quad q_1 \quad q_2 \quad q_3 \; \ldots \; q_n \quad]^T \text{ or } Q_{N\times 1} = (X_{6\times 1} \quad q_{6\times 1}) \tag{2-1}$$

where:

$X = (x, \quad y, \quad z, \quad \theta, \quad \varphi, \quad \psi\,)$ = defines the "main body" (the absolute position),

$q = (q_1, \ldots . q_n\,)$= represent joint angles.

The dynamic model has the matrix form:

$$H(Q)\ddot{Q} + h(Q, \dot{Q}) = T \tag{2-2}$$

where:

$T_{Nx1} = (0, \ldots, 0, \tau_1, \ldots, \ \tau_n)$=($0_{6x1}, \tau_{n\times 1})$ = the generalized vector of drives,

$\tau = (\,\tau_1 \ldots \tau_n)$ = the joint torques,

$H_{N\times N}$ = is the inertial matrix, capturing the system's mass distribution and its response to acceleration

$h_{N\times 1}$ = incorporates the effects of gravity, centrifugal forces, and Coriolis' forces.

Equation 2, serves as the foundation for analyzing the dynamic behavior of robotic systems, allowing the prediction and control of their motion accurately.

The contacts (one or more) with the environment are now introduced. Contact refers to a particular robot link and restricts the relative motion of that link with the relevant environmental object. If there are m restricted directions, the contact is expressed as:

$$s^c(Q, Q_b) = 0 \tag{2-3}$$

where s^c is the vector of relative link-to-object position, which depends on the robot position Q (of dimension N) and the object position Q_b (of dimension k). By first and second derivation:

$$\dot{s}^c = J(Q, Q_b)\dot{Q} + J_b(Q, Q_b)\dot{Q}_b = 0 \tag{3a}$$

$$\ddot{s}^c = J(Q, Q_b)\ddot{Q} + J_b(Q, Q_b)\ddot{Q}_b + A\big(Q, \dot{Q}, Q_b, \dot{Q}_b\big) = 0 \tag{3b}$$

where:

$J = \frac{\partial s^c}{\partial Q}$ and $J_b = \frac{\partial s^c}{\partial Q_b}$ are Jacobeans of dimensions $m \times N$ and $m \times k$ respectively, and A = contains second partial derivatives.

Contact introduces reaction forces and moments. Reactions appear along the restricted directions sc. Let $R\, m \times 1$ be the vector of reactions.

The dynamics of the contact motion is now described by the model:

$$H(Q)\ddot{Q} + h\big(Q, \dot{Q}\big) = T + J^T\big(Q, \dot{Q}_b\big)R \tag{2-4a}$$

$$\ddot{s}^c = J(Q, Q_b)\ddot{Q} + J_b(Q, Q_b)\ddot{Q}_b + A\big(Q, \dot{Q}, Q_b, \dot{Q}_b\big) = 0 \tag{2-4b}$$

$$W(Q)\ddot{Q}_b + w\big(\,Q_b, \dot{Q}_b\big) = T_b - J_b^T(Q, Q_b)R = 0 \tag{2-4c}$$

$$\bar{\bar{H}}\ddot{\theta} + \bar{\bar{h}}(Q, \dot{Q}, \theta^a, \dot{\theta^a}, \theta^b, \dot{\theta^b}) = C \cdot u \tag{2-4d}$$

The model (4) contains the robot dynamics (N-dimensional sub-model (4a)), the object dynamics (k-dimensional sub-model (4c) with model matrices Wkxk and wkx1), and the geometry of contact (m-dimensional subsystem (4b)). Equation (14d) describes dynamics of the antagonistically coupled drives including motors and gearboxes. It relates the control inputs (u_{2nx1} antagonistic motors voltages for the robot and T_b driving torque for the object) to the motion ($Q_{N\times 1}$, $\theta_{2n\times 1}$ and $Q^b_{k\times 1}$ for the robot, antagonistically coupled motors and the object respectively) and the contact reactions ($R_{k\times 1}$). The matrices $H, W, w, \bar{\bar{H}}$ and $\bar{\bar{h}}$, are robot's inertial matrix; matrix that takes care of gravity, centrifugal, Coriolis' effects, and joint geometry; inertial matrix of the object; similar effects referring to object; two matrices describing dynamics of the antagonistically coupled drives respectively. The vector s^c represents constrained coordinates due to in contact motion, while the J , J_b, and A, are appropriate Jacobians and adjoined matrix.

Consider motion of the contacted object (in this case mobile wheeled base) as prescribed - Q_b, the object dynamics is omitted and model becomes:

$$H(Q)\ddot{Q} + \tilde{h}\big(Q, \dot{Q}, \theta^a, \dot{\theta^a}, \theta^b, \dot{\theta^b}\big) = J^T(Q, Q_b)R \tag{2-5a}$$

$$\ddot{s}^c = J(Q, Q_b)\ddot{Q} + J_b(Q, Q_b)\ddot{Q}_b + A\big(Q, \dot{Q}, Q_b, \dot{Q}_b\big) = 0 \tag{2-5b}$$

$$\overline{\overline{\mathrm{H}}}\ddot{\theta} + \bar{\bar{h}}(Q, \dot{Q}, \theta^a, \dot{\theta^a}, \theta^b, \dot{\theta^b}) = \mathrm{C} \cdot \mathrm{u} \tag{2-5c}$$

The model (5) enables integration of the system and therefore simulation of the anthropometric robot on the mobile base. This means that for given control voltages u and knowing object motion Q_b, one can calculate robot motion Q, motor positions θ and reaction forces/torques $\boldsymbol{R}$.

Therefore, the target configuration of the anthropometric robot moving on the four wheeled mobile base is tested, and examination of the cart design and movement limits are carried out using derived model.

The kinematic equations of the four-wheeled mobile base describe the relationship between the vehicle's motion and its orientation angles. These equations are essential for understanding the vehicle's trajectory and steering behavior. The kinematic equations of the four wheeled mobile base are presented with model equations 6:

$$\dot{x}_e = V\cos(\psi + \beta) \tag{2-6a}$$

$$\dot{y}_e = V\sin(\psi + \beta) \tag{2-6b}$$

$$\dot{\psi} = \frac{V\cos\beta}{l_f + l_r} tg\delta \tag{2-6c}$$

where:

V = velocity of center of gravity (c.g.) of the vehicle which is at point C,

ψ = yaw angle (orientation angle with respect to global coordinate x_e),

β is vehicle slip angle,

$\chi = \psi + \beta$ = defines the total orientation angle

$\dot{\psi} =$ an angular velocity represents the rate of change of the vehicle's orientation angle

δ is the steering angle of front wheels

l_f and l_r are the distances of points A and B from the vehicle's center of gravity, respectively.

$l = l_f + l_r$ represents the total length of the vehicle

Dynamic model (2-7), can be derived from Figure 2. The equations describe the forces and moments acting on the vehicle, influencing its motion and stability. Model of dynamic motion consist two force balance equations (2-7a and 2-7b) and Moments Balance (equation 2-7c). The Forces Balance describe the forces acting along the system axes and the moments balance equation describes the rotational motion of the vehicle around the z-axis, normal to the plane C_{xy}.

$$m(\dot{V}_x - V_y\dot{\psi}) = -F_f\sin\delta + F_D \tag{2-7a}$$

$$m(\dot{V}_y - V_x\dot{\psi}) = -F_f\cos\delta + F_r \tag{2-7b}$$

$$J\ddot{\psi} = l_f F_f \cos\delta - l_r F \tag{2-7c}$$

where:

m = mass of the vehicle

J = inertial moment of the vehicle around the mass center,

F_D = driving force on the rear axis - along x axis,

F_f and F_r = resultant side forces on the front and the rear wheel.

F = the total force acting on the vehicle.

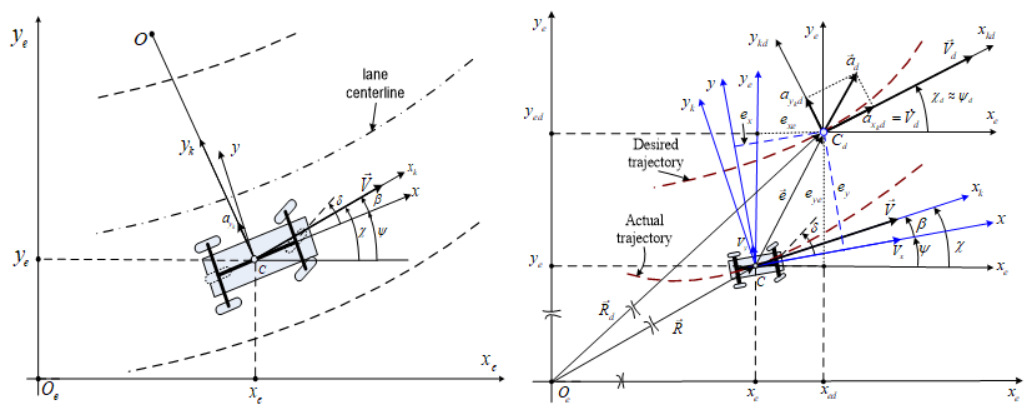

Figure 2. Kinematics of lateral motion and tracking reference (desired) trajectory with a mobile robot.

3. Simulation Results

The typical cart movements are examined.

During these cart movements the robot has task to keep a prescribed position (up-right torso position with bent elbows for 15^0 and outstretched forward arms for 30^0).

- Linear (longitudinal)
- lateral acceleration and
- Circular movement (alternatively, left and right turns)

There are three phases in this motion: acceleration and deceleration take 40% of the total task time (equally divided, 20%+20%) and the rest of the time (60%) the cart moves with constant velocity. So, this is trapezoidal velocity profile.

Table 1. Characteristics of the cart longitudinal and lateral motions

Parameters	Longitudinal trapez. motions	Lateral trapez. motions
Distance (m)	2	2
Time (s)	2.2	2.3
Acceleration (m/s^2)	2.583	2.363
max Velocity (m/s)	1.84	1.45
max x_{ZMP} (cm)	0.3 (min); 5.6(max)	2.2 (min); 2.5(max)
max y_{ZMP} (cm)	-0.9 (min); 0,1(max)	-2 (min); 2.2(max)
*Cart dim. a (cm)	26	20

Note. *Cart a dim (cm) —min.cart dimension

For testing, we used the fixed length of the cart motion – a distance of $2m$. Different values of acceleration (and accordingly different motion durations) were checked. Good results (satisfactory robot behavior) were obtained for a time of $2.2s$ or longer (*i.e.* acceleration or less). Satisfactory behavior means robot stability. If we reduced the time (thus increasing acceleration) the robot would become instable. The consequence of instability is that the robot falls over. An explanation for such an inappropriate robot reaction is that too high acceleration causes strong inertial forces; the drive in the waist Y joint (controller and DC motors) is not sufficiently strong to keep the waist and the torso in the upright position.

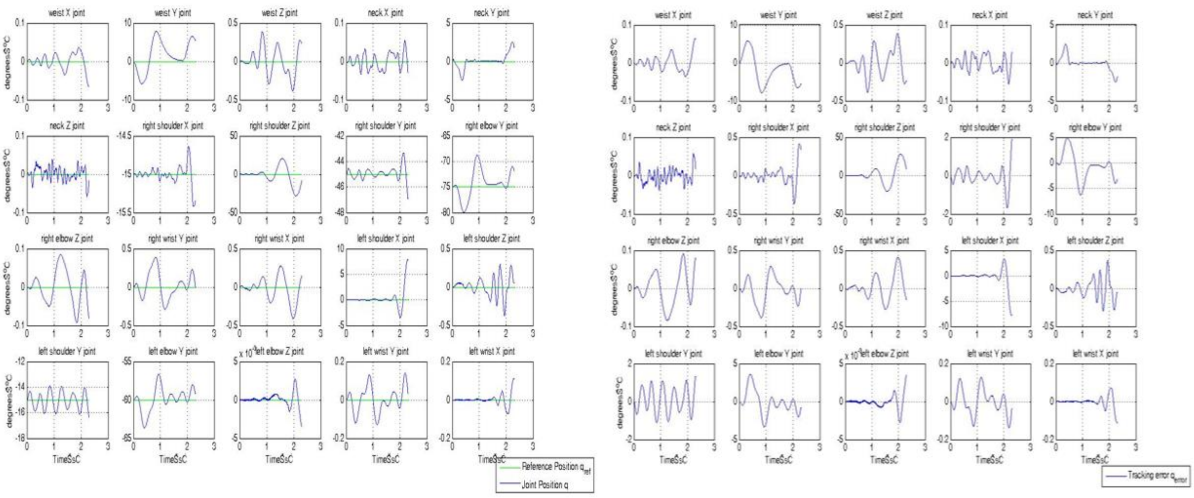

Figure 3. The position of robot joints and tracking errors by longitudinal (linear) acceleration of the cart.

In Figure 3 the time histories of the robot joint positions during the linear cart motion are shown. It can be seen that the strongest influence is on the Y joints, as we expected.

Robot tracking errors are also presented in Figure 4 (right). The waist Y joint and right elbow Y joint are the most illustrative examples of disturbance influence (max. deviation is approximately -75^0). Still, this is inside of the stability margins. The joints other than Y have a practically negligible problem in tracking references.

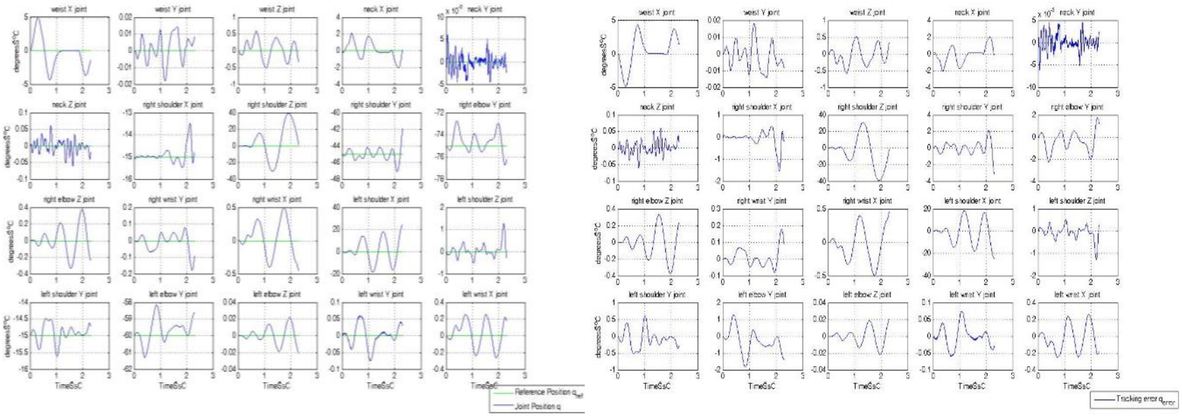

Figure 4. The position of robot joints and tracking errors by lateral trapezoidal movement of the cart.

If we compare with the previous movement for the same size of amplitude of 1m, and a time of 2.5s, the influence of external disturbances does not change. But for 1m, and time 3s the distribution of a quantity of forces is very similar with oscillatory motion in longitudinal direction forward-backward. Characteristics of the lateral oscillatory acceleration by impulse and long-term forces are given in table 2.

Table 2. Characteristics of the lateral oscillatory acceleration by impulse forces and by long-term forces with A=1m, T=3s.

A=1 T=3 s	By impulse forces					By long-term forces				
		Zmp X		Zmp Y		A=1 T=3 s	Zmp X		Zmp Y	
Direction [deg]	$F_{max\ I-}$ [N]	min	max	min	max	$F_{max\ II}$ [N]	min	max	min	max
0	F=1500N	-1,7	2,5	-1,6	1,2	F=100N	0,6	2,5	-1,7	1,3
22.5	F=1500N	-1,2	2,5	-1,4	1,9	F=150N	-5,5	2,5	-2	2
45	F=1000N	1,3	2,5	-1,2	2,9	F=80N	2,1	2,5	-1,4	2,2
67.5	F=1000N	2	2,5	-1,5	5,7	F=50N	2,4	2,5	-1,3	1,9
90	F=1000N	2	2,5	-3	7,7	F=50N	2,2	2,5	-1,7	1,2
112.5	F=1000N	2,3	3,2	-1,5	5,7	F=50N	2,1	2,6	-0,8	1,3
135	F=1500N	2,3	5,3	-5,1	8,5	F=80N	2,4	3	-1,4	2
157.5	F=1500N	2	6,5	-1,5	2	F=120N	2,5	7,3	-1	1,3
180	F=1500N	2	7,5	-1,8	1,2	F=120N	2,5	10,5	-1	1

A-amplitude; T-time

Combined oscillatory motion simulates a situation where the robotic platform moves along a circular trajectory (alternatively, left and right turns): the intention is to combine longitudinal accelerations and decelerations with centrifugal side effects. The characteristics for a circular motion with an amplitude of 1m and an approach of 3.5s are presented in Table 3.

Table 3. Characteristics of the cart circular trajectory (alternatively, left and right turns)

Parameters	Circular trajectory
Distance (m)	1
Time (s)	3.5
Acceleration (m/s^2)	6,445
max Velocity (m/s)	1.84
max x_{ZMP} (cm)	-3.7 (min); 10.6(max)
max y_{ZMP} (cm)	-4 (min); 3,3(max)
*Cart dim. a (cm)	56

Note. *Cart a dim (cm) —min. cart dimension

Figure 5 shows the position of the joints of the robot for simulations of a circular movement with a radius of 1m and a time period of T=3.5s.

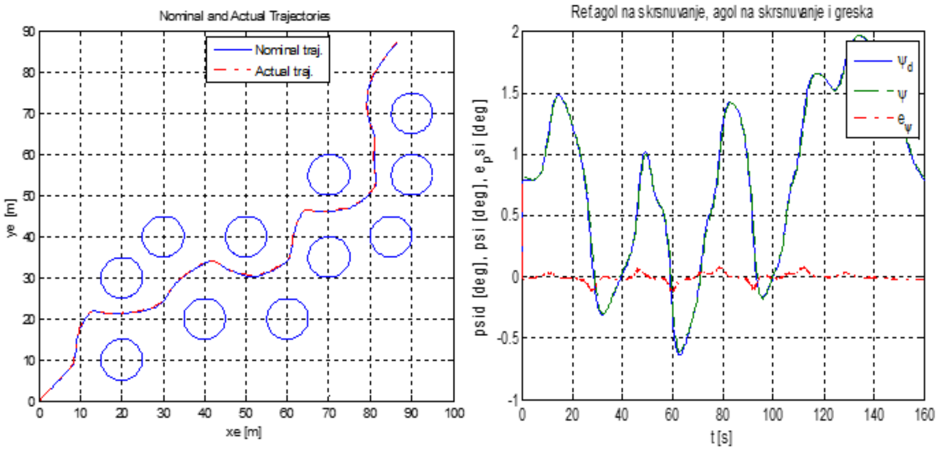

Figure 5. Robot course angle following during the movement along referent trajectory and referent trajectory following ψ_d - nominal angle, ψ - real angle, e_ψ tracking error.

4. Discussion

The results obtained from the simulation demonstrate the commendable stability of the robot across various cart movements, encompassing linear and lateral trapezoidal motions, as well as circular trajectories. These findings resonate with previous research, such as Han and Kim's study on posture-stabilizing control of quadruped robots utilizing a cart-inverted pendulum model, highlighting a shared emphasis on stability enhancement in robotic systems [27]. Additionally, the intermittent feedback-control strategy proposed by Yoshikawa et al., drawing an analogy to human stick balancing, aligns with the effective regulation of movements observed in our robot's system [28]. Furthermore, Morasso et al.'s work aimed at improving intermittent feedback strategies to match human performance limits in stabilizing a cart inverted pendulum underscores the importance of robust control algorithms in achieving stable robotic behaviors across diverse tasks, echoing the findings of our study [29].

Moreover, the stability demonstrated by the mobile robot during diverse cart movements finds resonance with recent literature in the field of mobile robotics. Borkar et al. conducted a comprehensive review of stability analysis and navigational techniques of wheeled mobile robots, stressing the significance of stable performance for effective navigation [30]. Similarly, the analysis of mobile robot stability through 3D dynamics and lumped parameter tire modeling by Jeong and Sohn provides further insights into critical stability aspects in mobile robotics [31]. By showcasing minimal deviations from desired positions across various motions, our study aligns with the broader discourse on stability in mobile robotics, emphasizing the importance of stable performance for navigating real-world environments and executing tasks effectively.

The analysis of the simulation data reveals a direct correlation between acceleration levels and robot behavior, wherein increased acceleration, achieved by reducing the duration of motion, compromises the robot's stability, potentially leading to instabilities and falls. This observation underscores the critical importance of balancing acceleration and motion duration to optimize robot performance while ensuring stability. Adhering to appropriate acceleration profiles can mitigate the risk of instability, thereby enhancing the overall reliability of the robot's operations.

Additionally, research on human understanding of robot motion highlights the role of velocity and orientation in shaping human perception, further emphasizing the importance of factors such as acceleration in robot behavior [32]. Furthermore, in the context of collaborative robotics, advancements and perspectives underscore the importance of addressing key technologies, including control algorithms regulating robot motion, to enhance collaboration between humans and robots [33].

Therefore, considering the broader literature, our findings contribute to a comprehensive understanding of the significance of acceleration in robot behavior and its implications for stability and performance optimization.

5. Conclusion

Finding the boundaries of the proposed control algorithm and establishing the cart dimensions to avoid the mobile robot (during different cart motions) from tipping-over was the topic of this research. Bearing in mind that the robot has compliant actuation (expandable tendons) makes it more sensitive to external influence. Any disturbance can cause oscillation accompanied by a specific and potentially highly risky situation – the resonance. Therefore, robust robot control was absolutely necessary to enable the examination of the complete anthropometric robot behavior on the mobile base and check its behavior in such disturbances.

As expected, the robot handles with low-speed cart movements, and intuitively problems appear with an increase in speed.

The analysis of the longitudinal and lateral motions of the cart revealed key characteristics such as acceleration profiles, maximum velocities, and corresponding robot joint responses. Trapezoidal velocity profiles were found to be effective in maintaining stability, with longer motion durations yielding more stable robot behavior.

Furthermore, the examination of lateral oscillatory acceleration due to impulse and long-term forces provided valuable insights into the robot's response to external disturbances. The analysis highlighted the importance of considering both the magnitude and duration of external forces in assessing the robot's stability.

Also, the mobile robot with low-speed guidance and control has been successfully simulated in an environment full of obstacles. The mobile robot has 4-wheels configuration, electric drive on the rear vehicles, and is directed from the front wheels. Simulation of movement is in a horizontal (x-y) plane and the dynamic modelling is 3-DOF system (system of three degrees of freedom).

The experiments have demonstrated that the stability of the robot can be preserved for some "reasonably" fast movements of the cart, relying on the appropriate cart design. The obtained results are encouraging and it proves that a compliant anthropometric mobile robot could be used to work in services—in homes, department stores, restaurants, museums, hospitals, etc., despite its very complex structure and demanding control requirements.

Overall, the findings from this study contribute to a better understanding of the mobile robot's capabilities and limitations in dynamic environments. Future research may focus on further optimizing control strategies and design parameters to enhance the robot's stability and performance in real-world applications.

References

[1] Licardo, J. T., Domjan, M., & Orehovački, T. (2024). Intelligent Robotics—A Systematic Review of Emerging Technologies and Trends. Electronics, 13(3), 542. https://doi.org/10.3390/electronics13030542.

[2] Jánoš, R., Sukop, M., Semjon, J., Tuleja, P., Marcinko, P., Kočan, M., Grytsiv, M., Vagaš, M., Miková, Ľ., & Kelemenová, T. (2022). Stability and Dynamic Walk Control of Humanoid Robot for Robot Soccer Player. Machines, 10(6), 463 https://doi.org/10.3390/machines10060463.

[3] Zhong, J., Ling, C., Cangelosi, A., Lotfi, A., & Liu, X. (2021). On the Gap between Domestic Robotic Applications and Computational Intelligence. Electronics, 10(7), 793. https://doi.org/10.3390/electronics10070793.

[4] Potkonjak, Veljko. (2020). Is Artificial Man Still Far Away: Anthropomimetic Robots Versus Robomimetic Humans. Robotics 9, no. 3: 57. https://doi.org/10.3390/robotics9030057.

[5] Antoska-Knights V, Gacovski Z, Stojce Deskovski S. (2017). Obstacles Avoidance Algorithm for Mobile Robots, Using the Potential Fields Method. Universal Journal of Electrical and Electronic Engineering, 5(4), 75-84. doi: 10.13189/ujeee.2017.050402,

[6] Ngwenya, T., Ayomoh, M., & Yadavalli, S. (2022). Virtual Obstacles for Sensors Incapacitation in Robot Navigation: A Systematic Review of 2D Path Planning. Sensors (Basel, Switzerland), 22(18), 6943. https://doi.org/10.3390/s22186943,

[7] Jin, J., & Chung, W. (2019). Obstacle Avoidance of Two-Wheel Differential Robots Considering the Uncertainty of Robot Motion on the Basis of Encoder Odometry Information. Sensors, 19(2), 289. https://doi.org/10.3390/s19020289,

[8] Moharam Habibnejad Korayem, H.N. Rahimi, A. Nikoobin. (2012). Mathematical modeling and trajectory planning of mobile manipulators with flexible links and joints. Applied Mathematical Modelling, 36(7), 3229-3244. https://doi.org/10.1016/j.apm.2011.10.002

[9] Liang, C.J., & Cheng, M. H. (2023). Trends in Robotics Research in Occupational Safety and Health: A Scientometric Analysis and Review. International Journal of Environmental Research and Public Health, 20(10), 5904. https://doi.org/10.3390/ijerph20105904,

[10] Berx, N., Adriaensen, A., Decré, W., & Pintelon, L. (2022). Assessing System-Wide Safety Readiness for Successful Human–Robot Collaboration Adoption. Safety, 8(3), 48. https://doi.org/10.3390/safety8030048,

[11] Antoska Knights, V., Stankovski, M., Nusev, S., Temeljkovski, D., & Petrovska, O. (2015). Robots for safety and health at work. Mechanical Engineering – Scientific Journal, 33 (3), 275-279.

[12] Antoska Knights, V., & Gacovski, Z. (2024). Methods for Detection and Prevention of Vulnerabilities in the IoT (Internet of Things) Systems. IntechOpen. doi: 10.5772/intechopen.113898.

[13] Antoska Knights V., Gacovski Z., Deskovski S., & Olivera Petrovska. (2018). Guidance and Control System for Platoon of Autonomous Mobile Robot. Journal of Electrical Engineering, 6(5), 281-288. doi: 10.17265/2328-2223/2018.05.000.

[14] Potkonjak V, Vukobratovic M, Babkovic K, Borovac B. (2007). Simulation Model of General Human and Humanoid Motion. Multibody System Dynamics, 2007; 17(1):71-96.

[15] Holland, O., & Knight, R. (2006). The Anthropomimetic Principle. In Proc. of the Symposium on Biologically Inspired Robotics edited by J. Burn and M. Wilson (AISB06), Bristol, UK.

[16] Antoska, V., Jovanović, K., Petrović VM, Baščarević N, Stankovski M. (2013). Balance Analysis of the Mobile Anthropomimetic Robot Under Disturbances – ZMP Approach. International Journal of Advanced Robotic Systems, 10(4). doi:10.5772/56238.

[17] Antoska-Knights V, Gacovski Z, Deskovski S. Obstacles Avoidance Algorithm for Mobile Robots, Using the Potential Fields Method. Universal Journal of Electrical and Electronic Engineering, 2017;5(4):75-84. DOI: 10.13189/ujeee.2017.050402.

[18] Kaur, A., Guo, T., Wang, J., Wang, Z., Chen, W., Chen, G., & Zhang, S. (2022). Research on Path Planning of Mobile Robot with a Novel Improved Artificial Potential Field Algorithm. Mathematical Problems in Engineering, 2022, 5692350. https://doi.org/10.1155/2022/5692350.

[19] Yang, L., Li, P., Qian, S., Quan, H., Miao, J., Liu, M., Hu, Y., & Memetimin, E. (2023). Path Planning Technique for Mobile Robots: A Review. Machines, 11, 980. https://doi.org/10.3390/machines11100980.

[20] Vukobratovic, M., Frank, A., & Juricic, D. (1970). On the stability of biped locomotion. IEEE Transaction on Biomedical Engineering, 17, 25-36.

[21] Kim, J., & Chung, W. (2002). Real-time ZMP Compensation Method using Null Motion for Mobile Manipulators. Proceedings of the 2002 IEEE International Conference on Robotics & Automation, Washington, DC, USA (Vol. 2, pp. 1967-1972).

[22] Vukobratovic, M., & Borovac, B. (2004). Zero-Moment Point—Thirty Five Years of its Life. International Journal of Humanoid Robotics, 1(1), 157–173.

[23] Wang, J., & Li, Y. (2009). Static Force Analysis for a Mobile Humanoid Robot Moving on a Slope. In IEEE International Conference on Robotics and Biomimetics (ROBIO08), Bangkok, Thailand (pp. 371-376).

[24] Wang, J., Li, Y., & Qiu, C. (2009). Analysis of Dynamic Stability Constraints for a Mobile Humanoid Robot. In IEEE International Conference on Robotics and Biomimetics (ROBIO08), Bangkok, Thailand (pp. 639-644).

[25] Razzaghi, P., Al Khatib, E., & Hurmuzlu, Y. (2019). Nonlinear dynamics and control of an inertially actuated jumper robot. Nonlinear Dynamics, 97, 161-176.

[26] Chignoli, M., Kim, D., Stanger-Jones, E., & Kim, S. (2021). The MIT Humanoid Robot: Design, Motion Planning, and Control for Acrobatic Behaviors. arXiv, arXiv:2104.09025.

[27] Han, KC., Kim, JY. (2003). Posture stabilizing control of quadruped robot based on cart-inverted pendulum model. Intel Serv Robotics 16, 521-536 (2023). https://doi.org/10.1007/s11370-023-00480-8.

[28] Yoshikawa N, Suzuki Y, Kiyono K, & Nomura T. (2016). Intermittent Feedback-Control Strategy for Stabilizing Inverted Pendulum on Manually Controlled Cart as Analogy to Human Stick Balancing. Front. Comput. Neurosci., 10:34. doi: 10.3389/fncom.2016.00034.

[29] Morasso P, Nomura T, Suzuki Y, & Zenzeri J. (2019). Stabilization of a Cart Inverted Pendulum: Improving the Intermittent Feedback Strategy to Match the Limits of Human Performance. Front. Comput. Neurosci., 13:16. doi: 10.3389/fncom.2019.00016.

[30] Borkar, Kailash Kumar, Turki Aljrees, Saroj Kumar Pandey, Ankit Kumar, Mukesh Kumar Singh, Anurag Sinha, Kamred Udham Singh, and Vandana Sharma. (2023). Stability Analysis and Navigational Techniques of Wheeled Mobile Robot: A Review. Processes 11, no. 12: 3302. https://doi.org/10.3390/pr11123302.

[31] Jeong, JS., Sohn, JH. (2023). Analysis of Mobile Robot Stability Through 3D Dynamics and Lumped Parameter Tire Modeling. Int. J. Precis. Eng. Manuf., 24, 1577-1585. https://doi.org/10.1007/s12541-023-00884-7.

[32] Papenmeier, F., Uhrig, M., & Kirsch, A. (2019). Human Understanding of Robot Motion: The Role of Velocity and Orientation. International Journal of Social Robotics, 11, 75-88. https://doi.org/10.1007/s12369-018-0493-4.

[33] Patil, S., Vasu, V., & Srinadh, K. V. S. (2023). Advances and perspectives in collaborative robotics: a review of key technologies and emerging trends. Discovery in Mechanical Engineering, 2(13). https://doi.org/10.1007/s44245-023-00021-8.